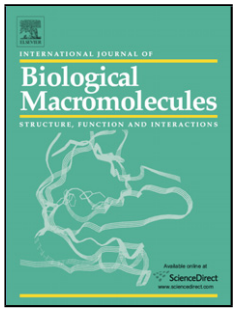

Title: Photopolymerized Maleilated Chitosan/Methacrylated Silk Fibroin Micro/nanocomposite Hydrogels as Potential Scaffolds for Cartilage Tissue Engineering

Authors: Yingshan Zhou, Kaili Liang, Shuyan Zhao, Can Zhang, Jun Li, Hongjun Yang, Xin Liu, Xianze Yin, Dongzhi Chen, Weilin Xu, Pu Xiao

PII: S0141-8130(17)34172-7
DOI: https://doi.org/10.1016/j.ijbiomac.2017.12.032
Reference: BIOMAC 8693

To appear in: *International Journal of Biological Macromolecules*

Received date: 25-10-2017
Revised date: 28-11-2017
Accepted date: 5-12-2017

Please cite this article as: Yingshan Zhou, Kaili Liang, Shuyan Zhao, Can Zhang, Jun Li, Hongjun Yang, Xin Liu, Xianze Yin, Dongzhi Chen, Weilin Xu, Pu Xiao, Photopolymerized Maleilated Chitosan/Methacrylated Silk Fibroin Micro/nanocomposite Hydrogels as Potential Scaffolds for Cartilage Tissue Engineering, International Journal of Biological Macromolecules https://doi.org/10.1016/j.ijbiomac.2017.12.032

Photopolymerized Maleilated Chitosan/Methacrylated Silk Fibroin Micro/nanocomposite Hydrogels as Potential Scaffolds for Cartilage Tissue Engineering

Yingshan Zhou [1, *], Kaili Liang [1], Shuyan Zhao [1], Can Zhang [1], Jun Li [1], Hongjun Yang [1], Xin Liu [1], Xianze Yin [1], Dongzhi Chen [1], Weilin Xu [1], Pu Xiao [2, *]

[1] Key Laboratory of Green Processing and Functional Textiles of New Textile Materials, Ministry of Education, Wuhan Textile University, Wuhan 430073, People's Republic of China

[2] Research School of Chemistry, Australian National University, Canberra, ACT 2601, Australia

Fax: +86-2759367690 Tel : +86-2759367690

Corresponding Authors: zyssyz@126.com; pu.xiao@anu.edu.au

Highlights:

- Photocrosslinkable water-soluble maleilated chitosan was synthesized.
- The composite hydrogels based on all-natural biomacromolecules were obtained by photopolymerization.
- The natural MCS/MSF composite hydrogels had the modulus comparative to articular cartilage and good biocompatibility to articular chondrocytes.

Abstract:

Hydrogels composed of natural materials exhibit great application potential in artificial scaffolds for cartilage repair as they can resemble the extracellular matrices of cartilage tissues comprised of various glycosaminoglycan and collagen. Herein, the natural polymers with vinyl groups, *i.e.* maleilated chitosan (MCS) and methacrylated silk fibroin (MSF) micro/nanoparticles, were firstly synthesized. The chemical structures of MCS and MSF micro/nanoparticles were investigated using Fourier transform infrared (FTIR) spectroscopy, proton nuclear magnetic resonance (^{1}H NMR) spectroscopy, and X-ray photoelectron spectroscopy (XPS). Then MCS/MSF micro/nanocomposite hydrogels were prepared by the photocrosslinking of MCS and MSF micro/nanoparticles in aqueous solutions in the presence of the photoinitiator Darocur 2959 under UV light irradiation. A series of properties of the MCS/MSF micro/nanocomposite hydrogels including rheological property, equilibrium swelling,

sol content, compressive modulus, and morphology were examined. The results showed that these behaviors could be tunable via the control of MSF content. When the MSF content was 0.1 %, the hydrogel had the compressive modulus of 0.32 ± 0.07 MPa, which was in the range of that of articular cartilage. The *in vitro* cytotoxic evaluation and cell culture of the micro/nanocomposite hydrogels in combination with mouse articular chondrocytes were also investigated. The results demonstrated that the micro/nanocomposite hydrogels with TGF-β1 was biocompatible to mouse articular chondrocytes and could support cells attachment well, indicating their potential as tissue engineering scaffolds for cartilage repair.

Keywords: Micro/nanocomposite hydrogel; chitosan; silk fibroin; photopolymerization; cartilage

1. Introduction

Articular cartilage injury is often caused by traumas, diseases and sport accident, and difficult to self-healing due to avascularity and a poor supply of repair cells around the tissue [1]. Even though a variety of current clinical treatments including autografts, allografts, mosaicplasty, and microfracture have been employed for cartilage defect repair [2], these treatments normally remain unsatisfactory and inefficient. Additionally, the clinical treatments still involve high risk of disease transmission [3].

One alternative strategy for dealing with cartilage damage is to develop tissue

engineered scaffolds. Hydrogel matrices have shown enormous potential as tissue engineering scaffolds for cartilage repair. The advantages of the scaffolds are mainly composed of hydrated environment similar to native tissues, network structure allowing the exchange of nutrients and metabolic wastes, ability to tune mechanical properties and most importantly, structural similarity to extracellular matrix in cartilage tissue, which promote cell adhesion migration and proliferation [4-6]. A number of approaches, such as ionic crosslinking [7], hydrogen bonding interaction [8], and covalent crosslinking [9] have been developed to fabricate the hydrogel scaffolds. Among these approaches, photo-triggered covalent crosslinking (photocrosslinking) technology has recently attracted increasing attentions due to the fast curing rate at physiological temperature, the low degree of invasiveness, and the temporal or spatial control for easy manipulation [10], which endows the fabricated hydrogels with unique morphologies and structures, favoring to control cellular behaviors [11]. And these characteristics are fatal to injectable hydrogels formed *in situ* in defected sites for cartilage repair.

Numerous synthetic and natural polymers, including poly (ethylene glycol) [12], gelatin [13], hyaluronic acid [14] and chitosan [15], have been currently employed for the fabrication of photocrosslinking hydrogels as tissue scaffolds for cartilage repair. However, hydrogels composed of synthetic materials are often bio-inert, while natural hydrogels are bioactive but mechanically inferior. And these are major limitations for cartilage tissue applications. To overcome these limitations, nanoparticles enhanced natural hydrogels were investigated [16-18]. Unfortunately, these nanoparticles

including nanoclay, nano-hydroxyapatite and nanosilicates are non-biodegradable.

To solve the abovementioned problems, in this study, we employed micro/nanoparticles based on natural polymers to reinforce natural hydrogels as scaffolds for cartilage repair. In view of bionics, we chose chitosan and silk fibroin micro/nanoparticles to prepare the hydrogel scaffolds by resembling the extracellular matrix of native cartilage. Chitosan, a naturally polysaccharide, is an attractive biopolymer for cartilage repair due to its biocompatibility, biodegradability, and most importantly, structural similarity to glycosaminoglycan found in cartilage, which can create a favorable chondrogenic microenvironment for cartilage tissue [19]. Silk fibroin, a naturally fibrous protein, is also a promising biomacromolecule for cartilage repair attributed to its biocompatibility, biodegradability and structurally mimicking the collagen architecture of native cartilage which promotes the growth of chondrocytes [20]. To prepare the photocrosslinkable hydrogels, chitosan and silk fibroin micro/nanoparticles were modified to attach highly reactive vinyl groups respectively, and then the photocrosslinked maleilated chitosan/methacrylated silk fibroin (MCS/MSF) micro/nanocomposite hydrogels were obtained via photopolymerization process under UV light irradiation using Darocur 2959 as the photoinitiator. A series of properties of the MCS/MSF hydrogels including rheological property, equilibrium swelling, morphology, sol content and compressive modulus were investigated. The in vitro cytotoxic evaluation and cell culture of the micro/nanocomposite hydrogels in combination with mouse articular chondrocytes were also studied to demonstrate their potential as tissue engineering scaffolds for

cartilage repair.

2. Experimental

2.1 Materials

Chitosan (CS, viscosity= 80 mpa·s, degree of deacetylation = 84.5 %) was obtained from Jinhu Crust Product Co., Ltd., China. Silk fibroin fiber was supplied from Yihongjuan textile Co., Ltd., Tongxiang, China, ball-milled into micro/nanoparticles. Maleic anhydride (MA) and 2-isocyanatoethyl methacrylate was supplied by Sinopharm Chemical Reagent Co, Ltd. and Adamas Reagent Co., Ltd., respectively. Darocur 2959 was donated from IGM Resins B.V. (Netherlands) and used as the photoinitiator for the photocrosslinking process. Recombinant human transforming growth factor-β1 (TGF-β1) was purchased from Peprotech Inc. (USA). Mouse articular chondrocytes (MACs) were obtained from Procell Life Scienc Co., Ltd., China. Other reagents were all A.R. grade.

2.2 Synthesis of water-soluble maleilated chitosan (MCS)

For further photopolymerization at physiological pH, a modified chitosan carrying vinyl carboxylic acid groups was designed and synthesized. Briefly, 1.0 g of chitosan was suspended in 110 mL of dimethyl sulfoxide (DMSO) with maleic anhydride (3.5 g) in the flask, and stayed for 24 h at 60 ℃. After that, saturated $NaHCO_3$ solution was added to the reaction mixture to adjust the pH to 8-9. The mixture was precipitated by acetone and then dialyzed (membrane molecular weight cut-off 12000

g·mol^{-1}) against water for 2 days. After that, the dialyzed solution was frozen at -40 ℃ for 24 h, and lyophilized for 48 h with the temperature about - 45 ℃ and vacuum degree below 10 Pa to obtain pure MCS. FTIR spectra and ^{1}H NMR spectrum was recorded on a Bruker Tensor 27 instrument and Bruker AV 400 NMR instrument (Bruker, Germany), respectively.

2.3 Synthesis of methacrylated silk fibroin (MSF) micro/nanoparticles

For photocrosslinking with MCS, silk fibroin micro/nanoparticles with vinyl group on the surface were prepared. Briefly, 2.0 g of silk fibroin micro/nanoparticles were dispersed in 60 mL dimethyl sulfoxide (DMSO). Then, 3.0 g of 2-isocyanatoethyl methacrylate was added and the reaction mixture was stirred for 12 h at 60 ℃. The mixture was precipitated by acetone and then dried under vacuum for 2 days and stored at -5 ℃ in the dark. X-ray photoelectron spectra were recorded on Shimadzu SPM-9700 instrument equipped with an Al-Kα radiation source (1486.6 eV).

2.4 Preparation of photopolymerized micro/nanocomposite hydrogels

A 6 % (w/v) MCS aqueous solution was prepared by dissolving 6.0 g MCS in 100 mL distilled water. MSF micro/nanoparticles were added into the MCS solution at weight ratio of 0.01% or 0.1% of MSF micro/nanoparticles to MCS solution, dispersed uniformly by stirring vigorously. D-2959 photoinitiator was added into the MCS/MSF solution at the concentration of 0.05 wt % (relative to amount of the solution). Here, D-2959, a water-soluble UV photoinitiator, was used in this study, as

it has been demonstrated to be the least cytotoxic to various cells [21]. Then, the blend solution was transferred into a disk-shaped mould consisting of two glass microslides separated by a spacer, and irradiated with an Omnicure Series 1000 UV light source (60 mW/cm^2, Exfo, Canada) for 30 min at ambient temperature. To obtain TGF-β1-containing micro/nanocomposite hydrogels, TGF-β1 solution was added to the MCS/MSF solution giving a final concentration of 50 ng/mL before the photocrosslinking process.

2.5 Rheological measurements

In situ dynamic photorheology [22] was applied to measure the elastic and viscous moduli during photopolymerization. A Haake Mars Rheometers (Thermo Fisher Scientific Inc.) equipped with a UV curing attachment and 20 mm parallel plate geometry was used to characterize the photocrosslinking kinetics. The upper plate was made of an optically transparent quartz acting as filter for UV light with a cut-off of 320-400 nm. The gap setting was fixed as 1.0 mm. Light intensity (60 mW/cm^2) was used for the crosslinking reaction of the precursor. Time-sweep oscillatory tests were performed at 25 ℃ at strain amplitude of 1.0 % and a 6.28 rad/s, which was within the linear viscoelastic region [23]. The storage and loss modulus values were continuously recorded by Haake RheoWin measuring and evaluation software.

2.6 Equilibrium water uptake

Lyophilized photopolymerized MCS/MSF micro/nanocomposite hydrogels

(weighted as W_1) were submerged in phosphate buffered saline (PBS) buffer solution (pH=7.4) at 37 ℃ for 48 h to reach swelling equilibrium. Swollen gels removed from the solution were dried superficially with filter paper, weighted as W_2. The equilibrium water uptake (EWU) was calculated as: $EWU = (W_2-W_1)/W_1$.

2.7 Sol determination

Sol content is an index reflecting the amount of the uncrosslinked macromolecules in hydrogels. It can be determined as follows: the lyophilized photocrosslinked MCS/MSF micro/nanocomposite hydrogels (dry mass recorded as m_0) were swollen three times in purified water at 37 ℃, with the water replaced every 12 h. The gels were again frozen, lyophilized and the final mass recorded as m_1. The sol content was calculated as: $sol = (m_0-m_1)/m_0$.

2.8 Mechanical test

Unconfined compression testing of photocured MCS/MSF micro/nanocomposite hydrogels was carried out on an Instron 5848 microtester (Instron, Norwood, MA, USA) with 10 kN load cell at a compression rate of 0.5 mm/min. The fracture stress and strain were determined with the failure point of the stress-strain curve, and the compressive strength was calculated. Three samples of each type of the hydrogels were examined in this experiment.

2.9 The morphology of the micro/nanocomposite hydrogels

To visually investigate the surface morphology of photocrosslinked MCS/MSF micro/nanocomposite hydrogels, a Jeol Model JSM-6510 scanning electron microscope (SEM) was used to analyze the pore structure. The freeze-dried samples were loaded on the surface of an aluminium SEM specimen holder and sputter coated with gold before observation. The accelerating voltage was 20 kV.

2.10 Cytotoxicity assays

To evaluate the cytotoxicity of the hydrogels toward to MACs, the sterilized photocrosslinked MCS/MSF micro/nanocomposite hydrogels with/without TGF-β1 were incubated in culture medium at extraction ratio of 1.25 cm^2/mL for 24 h at 37 ℃, after which the hydrogels were removed and the extraction medium was obtained.

200 μL of MACs suspension was seeded in 96–well plate at a concentration of 10^5 cells/well. After incubation at 37 ℃ for 1 day, the culture medium was instead of the extraction medium. After 1 day, the extract was removed and 20 μL of MTT solution was added to each well. MACs were allowed to incubate at 37 ℃ (5 % CO_2) for 4 h, and then the formazan reaction products were dissolved in dimethyl sulfoxide (150 μL) and the plates were shaken for 10 min. The optical density of the formazan solution was read on an ELISA reader at 568 nm.

The Dulbecco's modified eagle medium/nutrient mixture F-12 (DMEM/F-12) containing 10 % fetal bovine serum (FBS) was used as negative control for toxicity.

Results are depicted as mean ± standard deviation. Significance between the mean

values was calculated using ANOVA one-way analysis (Origin 7.0 SRO, Northampton, MA, USA). A value of $p < 0.05$ was considered as significant ($n = 6$).

2.11 Cell culture and cell morphology

To evaluate the behavior of MACs on/within MCS/MSF micro/nanocomposite hydrogels, a cell attachment/proliferation, study was carried out. TGF-β1 loaded MCS/MSF micro/nanocomposite hydrogels were cultured in DMEM/F-12 culture medium with MACs at a density of 10^6 cells/mL. After incubation at 37 ℃ for 2 day, cellular constructs were harvested, rinsed twice with PBS to remove non-adherent cells, and subsequently fixed with 4.0 % paraformaldehyde at 4 °C for 2 h. Then, the samples were lyophilized and sputtered with gold for observation by SEM.

3. Results and Discussion

3.1 Synthesis of MCS and MSF micro/nanoparticles

Chitosan is actually insoluble in water at physiological pH, which limits it from being widely used in many biomedical applications as tissue engineering scaffolds, drug carriers for controlled release, and genetic materials [24]. To improve the solubility of chitosan in water and facilitate the further photocrosslinking process, chitosan was modified by high hydrophilic carboxyl group and vinyl group to its reactive amino or hydroxyl groups. Here, chitosan was reacted with maleic anhydride to obtain water-soluble MCS. Vinyl groups on the side chain gave MCS a chance to further crosslinking to form network hydrogels. FTIR analysis was used to confirm

maleoyl modification of chitosan. For chitosan, typical characteristic absorption peaks can be observed, *e.g.* C=O stretching (1653 cm^{-1}), N-H bending (1599 cm^{-1}), glucosamine units (1082 cm^{-1}, 1028 cm^{-1}, and 897 cm^{-1}), similar to those reported in the literature [25]. After maleoylation, the FTIR spectrum of MCS shows absorptions at 3074 cm^{-1}, 1713 cm^{-1}, and 810 cm^{-1} [Figure 1 (a)], which are indicative of carbon hydrogen bonding (vinyl), the carbonyl group and double bond (vinyl) of the maleoyl groups, respectively. It verified the success of maleoyl functionalization of MCS. ^{1}H NMR of MCS and chitosan are illustrated in Figure 1 (b). Maleoylation is achieved as evidenced by peaks arising at δ = 6.2-6.5 ppm and 5.6 ppm assigned to N-maleoyl alkene protons. Their appearance confirmed the success of the maleoyl substitution of CS. The degree of maleoyl substitution (DS) of MCS was calculated by comparing integration of the vinyl protons (CH=CH-COO-) at 5.6 ppm with integration of the methyl protons (–$NHCOCH_3$) at 1.7 ppm: $DS= 3\times0.155\times I_{5.6}/I_{1.7}$. By calculation, DS was 1.67 for MCS, which was significantly higher than that reported in the literature [25]. Other peaks were assigned, *i.e.* 4.3 ppm for H-1 of GlcNAc and 3.3-3.6 ppm for H-3,4,5,6 of N-alkyl group, GlcN and GlcNAc. In addition, the peak at 2.8 ppm (H-2 proton for the deacetylated residues) was almost disappeared, which showed that most of -NH_2 group of chitosan was reacted with maleic anhydride. Maleilated chitosan could be dissolved in the deionized water, and the maximum concentration could reach to 8.0 % (w/v).

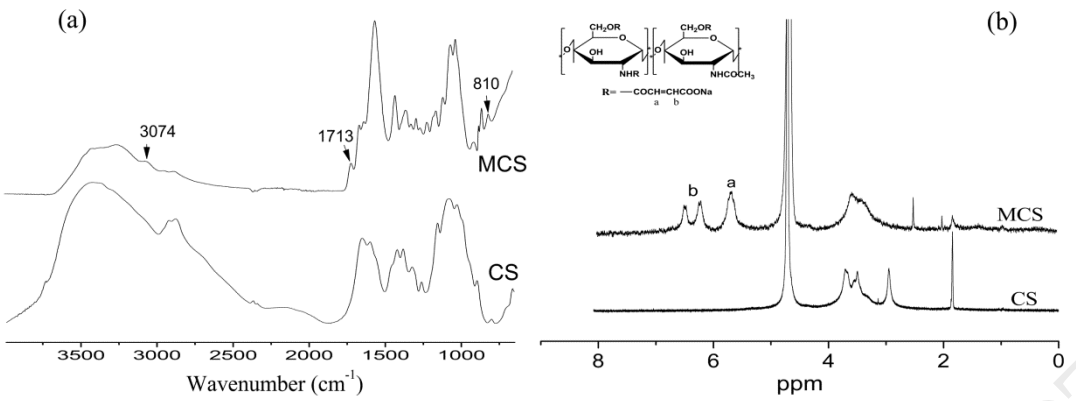

Figure 1. (a) FTIR and (b) NMR spectra of CS and MCS.

As a main crosslinking point of micro/nanocomposite hydrogels, silk fibroin (SF) micro/nanoparticles were selected to be modified with reactive polymerizable moieties for the photocrosslinking with MCS. SF micro/nanoparticles have many amino and hydroxyl groups, which are reactive sites for isocyanates. Herein, 2-isocyanatoethyl methacrylate was used to react with SF micro/nanoparticles to obtain MSF micro/nanoparticles. And dimethyl sulfoxide was used as a catalytic agent for the reaction [26]. The characteristics functional groups in SF and MSF micro/nanoparticles are presented in FTIR spectra as shown in Figure 2 (a). SF micro/nanoparticles have the characteristic peaks at 1655 cm^{-1} (amide I), 1535 cm^{-1} (amide II), 1236 cm^{-1} (amide III). After nucleophilic addition reaction, the FTIR spectrum of MSF micro/nanoparticles showed absorptions at 1702 cm^{-1} and 814 cm^{-1}, which are indicative of the carbonyl group and the double bond (vinyl) of the methacrylate group, respectively. Their appearance confirmed the success of the methacryl substitution of SF. It can be observed that, the peaks 1655 cm^{-1}, 1535 cm^{-1}, and 1236 cm^{-1} shift to 1625 cm^{-1}, 1522 cm^{-1}, and 1230 cm^{-1}, respectively after

methacryl reaction, which are probably attributed to conformational transition of SF [27].

The chemical component of SF and MSF micro/nanoparticles surface layers are determined by X-ray photoelectron spectroscopy. The high resolution C_{1s} spectra are displayed in Figure 2 (b) and 2 (c). By Gaussian peak-fitting, the carbon C_{1s} spectrum of SF micro/nanoparticles was deconvoluted into three sub-peaks. The sub-peaks at 284.5 eV, 286.0 eV, and 287.8 eV are contributed to carbons in C-H/C-C, C-N/C-O and C=O/N-C=O groups, respectively [28]. After methacrylation, the XPS spectrum for MSF micro/nanoparticles shows new peaks at 289.0 eV, which are attributed to O-C=O [28]. By calculation of peak area ratio (A_{289}/A_{total}), the degree of methacrylate substitution was 1.2 %. XPS results reconfirmed the success of the methacryl substitution of SF micro/nanoparticles.

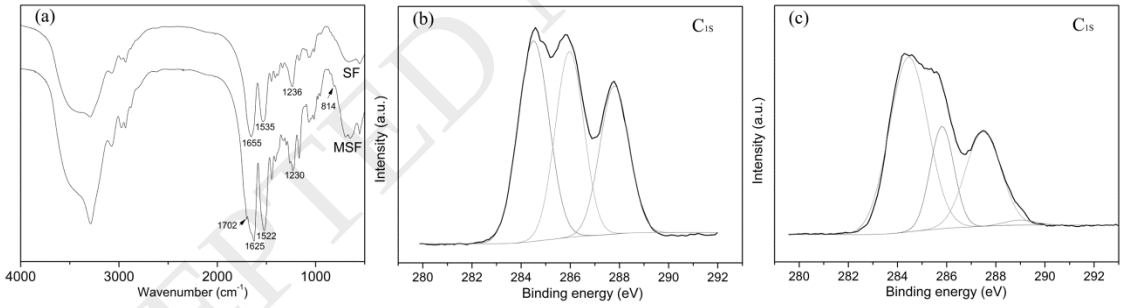

Figure 2. FTIR and XPS spectrum of SF and MSF. (a) FTIR of SF and MSF; (b) XPS of SF; and (c) XPS of MSF.

3.2 Rheological study

The schematic of photopolymerizable MCS/MSF hydrogels formation is exhibited in Fig. 3(a). To further investigate the photopolymerization process, in situ photo

rheology was applied. This method can monitor the change in modulus during the sol to gel transition in photopolymerizable hydrogel precursors [29], which can reflect the formation of hydrogel and crosslinking density [30]. Figure 3(b) shows photo rheology of MCS/MSF micro/nanocomposite hydrogels with different MSF contents. All the samples exhibit typical process of gelatin. The solutions start to gel (gel point) when G' = G", and photopolymerization reactions are finished when plateau modulus are reached. For pure MCS hydrogel, onset of gelation occurred at 276 s. However, gelation point of MCS/MSF micro/nanocomposite hydrogels increased from 340 s to 561 s with MSF content raised from 0.01 % to 0.1 %, which indicated that the MSF content affected the network formation. And it can be ascribed to the step mechanisms of free radical crosslinking [31]. More specifically, the addition of MSF led to higher viscosity of blend solutions, limiting the mobility of radicals and subsequently decreasing the rate of reaction. It can be also seen that, when MSF content increased from 0.01 % to 0.1 %, elastic modulus (gel point) increased from 1505 Pa to 2012 Pa, indicating an increased crosslinking density. Generally, it indicated that MSF content could influence the onset of gelation and the crosslinking density of the network.

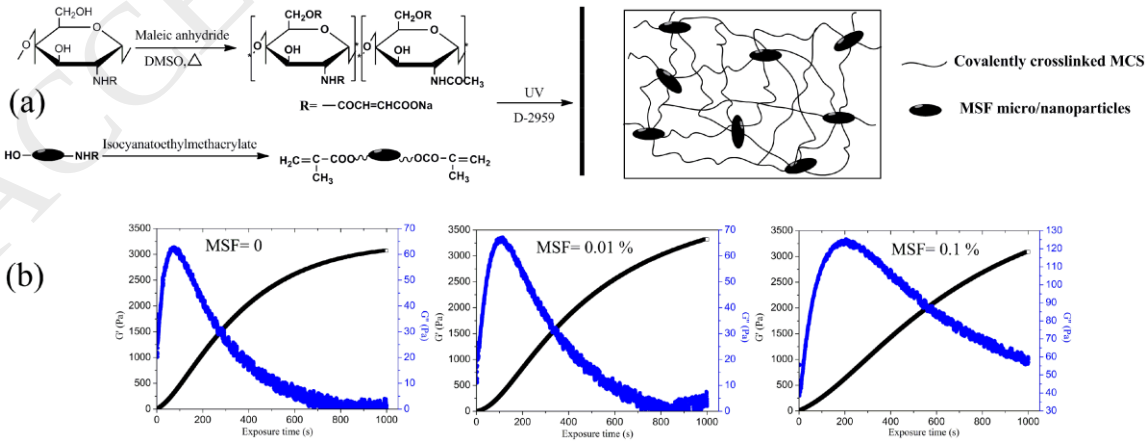

Figure 3. Reaction schematic (a) and photorheology (b) of MCS/MSF

micro/nanocomposite hydrogels.

3.3 Equilibrium water uptake and sol content

The equilibrium water uptake (EWU) and sol content of different MCS/MSF micro/nanocomposite hydrogel formulations were characterized and the results are summarized in Table 1. As illustrated, all the MCS based hydrogels exhibited high levels of equilibrium water uptake (> 8.0 times), obviously higher than that of other hybrid chitosan hydrogels (< 2.0 times) reported previously [32]. In this study, MCS is of anionic nature with hydrophilic carboxylate group in the molecular chain. In the alkaline environment, the dominant charges in the hydrogels were dissociated carboxylate group, which repelled electrostatically between molecules to form a loose network structure, leaving more water molecules to diffuse easily into the network and thus demonstrating high swelling.

When the level of MSF micro/nanoparticles increased, equilibrium water uptake of the micro/nanocomposite hydrogels decreased from 13.49 ± 0.93 to 8.79 ± 0.71. Meanwhile, sol content, an index reflecting the amount of the uncrosslinked macromolecules, declined significantly from 0.18 ± 0.01 to 0.10 ± 0.03, along with the increase of MSF content. It can be probably ascribed to the increase of the crosslinking density in the MCS/MSF micro/nanocomposite hydrogel system when MSF micro/nanoparticles content increased. Higher crosslinking density leads to a denser structure, which is helpful to hold the water content [33]. Equilibrium water content of MCS/MSF micro/nanocomposite hydrogels, calculated by the following

formula: $(W_2-W_1)/W_2 \times 100$ %, ranges from 86.0 % to 91.1 %, which is a little higher than that of the natural cartilage [34].

3.4 Mechanical properties of the hydrogels

Pure MCS hydrogel was very brittle and stiff, which was not suitable for the application as a tissue scaffold. Herein, MSF micro/nanoparticles were chosen to incorporate into MCS hydrogel for improvement of mechanical property. The mechanical properties of MCS/MSF micro/nanocomposite hydrogels are listed in Table 1. It can be seen that, compressive modulus of MCS/MSF micro/nanocomposite hydrogels increased as MSF content raised. It can be attributed to the fact that MSF micro/nanoparticles acted as main crosslinking points to crosslink the MCS macromolecules by reaction between methacrylate groups on the micro/nanoparticles surface and maleoyl groups of MCS molecular chain, which led to improvement of crosslink density and therefore enhancement of compressive strength. Moreover, the formation of hydrogen bond between -COOH of MCS and -OH or $-NH_2$ of MSF might contribute to the improved mechanical strength, similar to those reported in the literature [35]. Notably, when MSF content reached to 0.1 %, the compressive modulus of the micro/nanocomposite hydrogels significantly raised to 0.32 ± 0.07 MPa, which was in the range of that of articular cartilage (0.1 - 2.0 MPa) [36], indicating the potential of MCS/MSF micro/nanocomposite hydrogels as cartilage repair materials.

Table 1. Formulations and characteristics of MCS/MSF micro/nanocomposite hydrogels.

No.	MSF content (%)	EWU (g/g)	Sol fraction (g/g)	Compressive strength (MPa)
1	0	13.49±0.93	0.18±0.01	0.06±0.01
2	0.01	10.33±0.29	0.13±0.03	0.05±0.01
3	0.1	8.79±0.71	0.10±0.03	0.32±0.07

3.5 The morphology of the micro/nanocomposite hydrogels

The microstructure of hydrogels is very important because it controls mass transport, favoring the delivery of biological moieties and regeneration of tissues within the hydrogels [37]. The representative microstructure images of MCS/MSF micro/nanocomposite hydrogels are shown in Figure 4. Surface SEM micrographs of lyophilized micro/nanocomposite hydrogels revealed that all hydrogels demonstrated three-dimensional porous morphology. The pore diameter of the hydrogels reduced gradually and the microstructure became dense and glazed when MSF content increased. In terms of cross-section of the micro/nanocomposite hydrogels, MSF micro/nanoparticles were closely embed in the MCS matrix and the network structure of hydrogels became relatively denser, followed by the slightly decreased porosity size (Figure 4b). SEM micrographs with magnifications (Figure 4c-d) shows that, MSF particles were irregular-shaped micro/nanoparticles existed inside the matrix with a size distribution from 300 nm to 5500 nm. The introduction of MSF micro/nanoparticles as "fillers" reinforced the MCS matrix with improvement of covalent crosslinking degree and hydrogen bond interaction. This might be the reason why the swelling capacity of MCS/MSF micro/nanocomposite hydrogels gradually

reduced and compressive strength gradually improved with MSF content raised.

3.6 Cytotoxicity assays

MTT assays were carried out to investigate cytotoxicity of MCS/MSF micro/nanocomposite hydrogels on MACs. As shown in Figure 5, there were statistically significant differences ($p < 0.05$) in the cell activity in comparison with negative control for MCS/MSF micro/nanocomposite hydrogels. However, compared to MCS hydrogels, MCS/MSF micro/nanocomposite hydrogels showed statistically significant differences ($p < 0.05$) in the cell activity, indicating addition of MSF favoring the cytocompatibility of the nanocomposite hydrogels. Although statistically significant differences ($p < 0.05$) were observed in the cell activity in comparison with negative control at MCS/MSF micro/nanocomposite hydrogels with TGF-β1, the

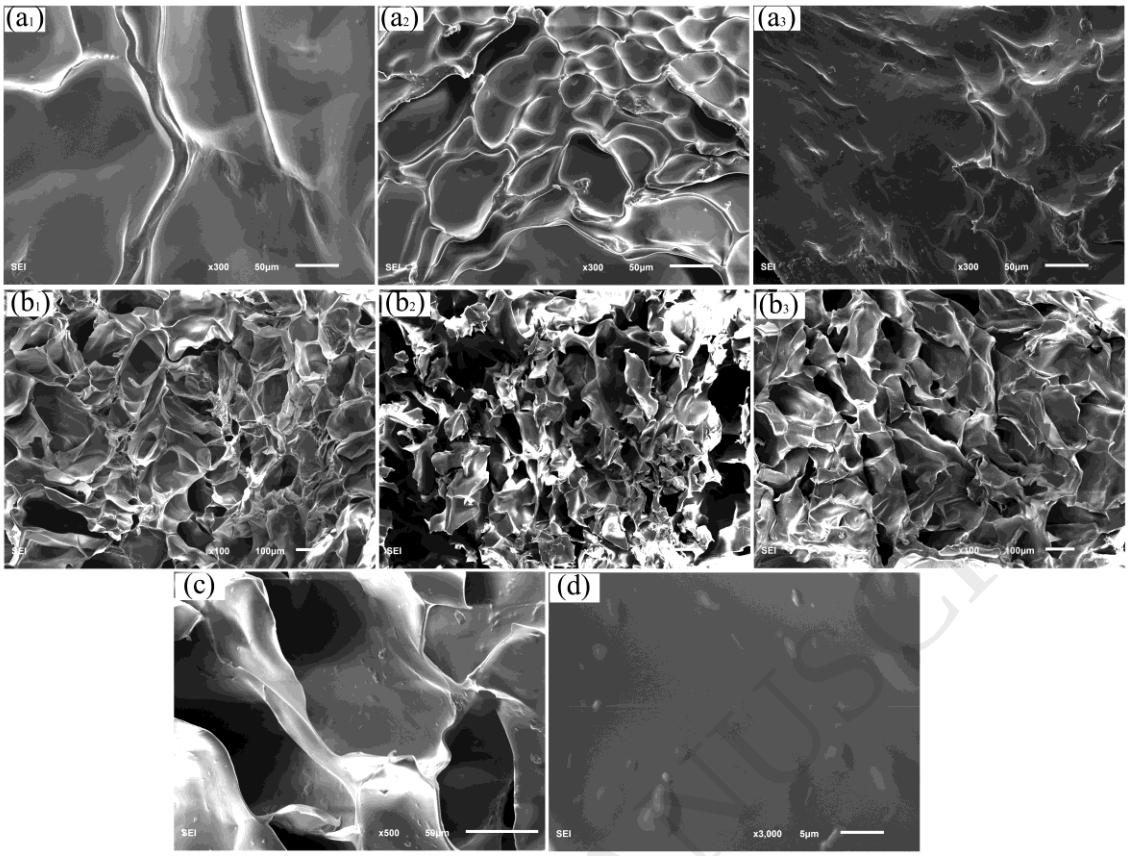

Figure 4. SEM micrographs of MCS/MSF micro/nanocomposite hydrogels with different MSF content. (1) 0; (2) 0.01 %; (3) 0.1 %. (a) Surface; (b) Cross-section; (c) Magnification of b_3, ×500; (d) Magnification of b_3, ×3000.

viability of the cell still reached 80 % of that of the negative control. According to International Standard ISO 10993-5 (2009), reduction of cell viability by more than 30 % is considered a cytotoxic effect. This indicates that photocrosslinked MCS/MSF micro/nanocomposite hydrogels with TGF-β1 were not toxic to MACs. Growth factors TGF-β1 could stimulate cell proliferation and promote osteochondral tissue regeneration [38, 39], and therefore its incorporation improved the cytocompatibility of the micro/nanocomposite hydrogels. The obtained results clearly suggested MCS/MSF micro/nanocomposite hydrogels with TGF-β1 were good candidates as

tissue engineering scaffolds for cartilage repair.

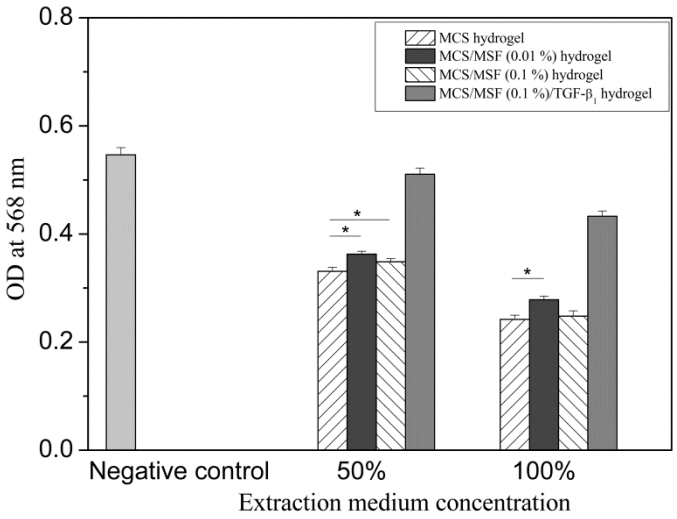

Figure 5. Cytotoxicity test of photocrosslinked MCS/MSF micro/nanocomposite hydrogels with negative controls ($p < 0.05$). *$p < 0.05$ was considered as significant.

3.7 Cell Morphology

MACs were used to study the cell behavior, *i.e.* investigate the general cell characteristics such as adhesion and evaluate the ability of micro/nanocomposite hydrogels to support cell growth and spreading. Specifically, the cell morphology in the MCS/MSF micro/nanocomposite hydrogels (MSF %= 0.1 %) with TGF-β1 was observed by SEM (Figure 6). It can be seen that, a relatively larger number of MACs attached on the pore wall of the surface of the micro/nanocomposite hydrogels with cell cluster in some areas, and closely connected each other. MACs exhibits near-spherical morphology, and cell cilium was clearly visualized on some cell surfaces. The results indicated that, the MCS/MSF micro/nanocomposite hydrogels with TGF-β1 can support MACs attachment *in vitro* well.

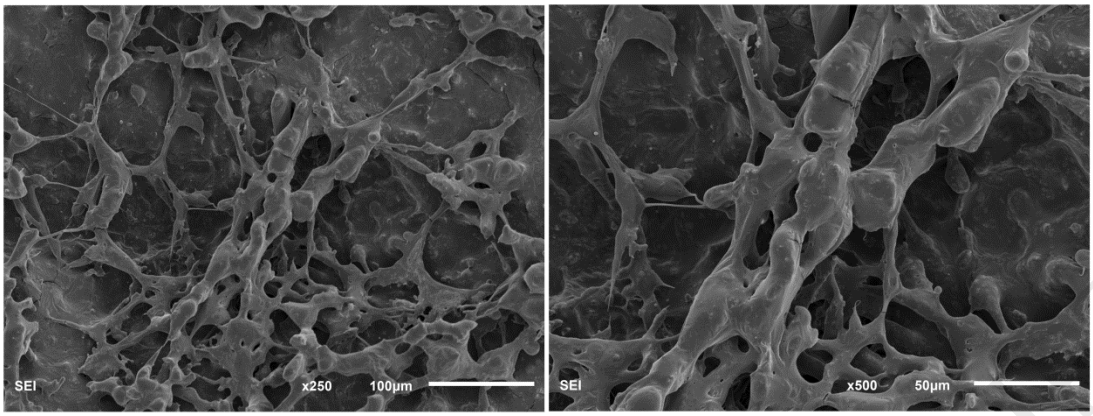

Figure 6. SEM images to show the MACs cultured in the MCS/MSF micro/nanocomposite hydrogels with TGF-β1.

4. Conclusions

Photocrosslinkable MCS/MSF micro/nanocomposite hydrogels were prepared from MSF micro/nanoparticles dispersed in MCS aqueous solutions by consequent photopolymerization process. EWU and sol content of the micro/nanocomposite hydrogels decreased with MSF content raised. The hydrogel exhibited the compressive modulus of 0.32 ± 0.07 MPa, which was in the range of that of articular cartilage. The in vitro cytotoxic evaluation and cell culture results showed the micro/nanocompsite hydrogels with TGF-β1 were biocompatible to mouse articular chondrocytes and could support cells attachment well, indicating their great potential as tissue engineering scaffolds for cartilage repair.

Acknowledgements

This study was supported by National Natural Science Foundation of China (Grant

No. 51203123, 51403165, 51503161) and the National Key Research and Development Program of China (No.2016YFA0101102).

References

[1] H. Park, B. Choi, J. Hu, M. Lee, Injectable chitosan hyaluronic acid hydrogels for cartilage tissue engineering, Acta Biomater. 9 (2013) 4779-4786.

[2] E. B. Hunziker, Articular cartilage repair: basic science and clinical progress. A review of the current status and prospects, Osteoarthr. Cartilage 10 (2002) 432-463.

[3] R. H. Koh, Y. Jin, B. Kang, N. S. Hwang, Chondrogenically primed tonsil-derived mesenchymal stem cells encapsulated in riboflavin-induced photocrosslinking collagen-hyaluronic acid hydrgel for meniscus tissue repairs, Acta Biomater. 53 (2017) 318-328.

[4] E. C. Beck, M. Barragan, M. H. Tadros, S. H. Gehrke, M. S. Detamore, Approaching the compressive modulus of articular cartilage with decellularized cartilage-based hydrogel, Acta Biomater. 38 (2016), 94-105.

[5] Y. Guo, T. Yuan, Z. Xiao, P. Tang, Y. Xiao, Y. Fan, X. Zhang, Hydrogels of collagen/chondroitin sulfate/hyaluronan interpenetrating polymer network for cartilage tissue engineering, J. Mater. Sci. Mater. Med. 23 (2012) 2267-2279.

[6] L. Bian, C. Hou, E. Tous, R. Rai, R. L. Mauck, J. A. Burdick, The influence of hyaluronic acid hydrogel crosslinking density and macromolecular diffusivity on human MSC chondrogenesis and hypertrophy, Biomaterials 34 (2013) 413-421.

[7] J. Y. Sun, X. Zhao, W. R. K. Illeperuma, O. Chaudhuri, K. H. Oh, D. J. Mooney, J.

J. Vlassak, Z. Suo, Highly stretchable and tough hydrogels, Nature 489 (2012) 133-136.

[8] Y. N. Chen, L. Peng, T. Liu, Y. Wang, S. Shi, H. Wang, Poly (vinyl alcohol)-tannic acid hydrogels with excellent mechanical properties and shape memory behaviors, ACS Appl. Mater. Interfaces 8 (2016) 27199-27206.

[9] S. L. Fenn, R. A. Oldinski, Visible light crosslinking of methacrylated hyaluronan hydrogels for injectable tissue repair, J. Biomed. Mater. Res. B Appl. Biomater. 104 (2016) 1229-1236.

[10] X. Gao, Y. Zhou, G. Ma, S. Shi, D. Yang, F. Lu, J. Nie, A water-soluble photocrosslinkable chitosan derivative prepared by Michael-addition reaction as a precursor for injectable hydrogel, Carbohydr. Polym. 79 (2010) 507-512.

[11] H. Aubin, J. W. Nichol, C. B. Hutson, H. Bae, A. L. Sieminski, D. M. Cropek, P. Akhyari, A. Khademhosseini, Directed 3D cell alignment and elongation in microengineered hydrogels. Biomaterials 31 (2010) 6941-6951.

[12] T. J. Klein, S. C. Rizzi, K. Schrobback, J. C. Reichert, J. E. Jeon, R. W. Crawford, D. W. Hutmacher, Long-term effects of hydrogel properties on human chondrocyte behavior, Soft Matter 6 (2010) 5175-5183.

[13] M. Bartnikowski, N. J. Bartnikowski, M. A. Woodruff, K. Schrobback, T. J. Klein, Protective effects of reactive functional groups on chondrocytes in photocrosslinkable hydrogel systems, Acta Biomater. 27 (2015) 66-76.

[14] J. W. S. Hayami, S. D. Waldman, B. G. Amsden, Photo-cross-linked methacrylated polysaccharide solution blends with high chondrocyte viability,

minimal swelling, and moduli similar to load bearing soft tissues, Eur. Polym. J. 72 (2015) 687-697.

[15] B. Choi, S. Kim, B. Lin, K. Li, O. Bezouglaia, J. Kim, D. Evseenko, T. Aghaloo, M. Lee, Visible-light-initiated hydrogels preserving cartilage extracellular signaling for inducing chondrogenesis of mesenchymal stem cells, Acta Biomater. 12 (2015) 30-41.

[16] R. Waters, S. Pacelli, R. Maloney, I. Medhi, R. P. H. Ahmed, A. Paul, Stem cell secretome-rich nanoclay hydrogel: a dual action therapy for cardiovascular regeneration, Nanoscale 8 (2016) 7371-7376.

[17] M. Sadat-Shojai, M. T. Khorasani, A. Jamshidi, 3-Dimensional cell-laden nano-hydroxyapatite/protein hydrogels for bone regeneration applications, Mater. Sci. Eng. C 49 (2015) 835-843.

[18] A. Paul, V. Manoharan, D. Krafft, A. Assmann, A. Uquillas, S. R. Shin, A. Hasan, M. A. Hussain, A. Memic, A. K. Gaharwar, A. Khademhosseini, Nanoengineered biomimetic hydrogels for guiding human stem cell osteogenesis in three dimensional microenvironments, J. Mater. Chem. B 4 (2016) 3544-3554.

[19] H. Tan, C. R. Chu, K. A. Payne, K. G. Marra, Injectable in situ forming biodegradable chitosan-hyaluronic acid based hydrogels for cartilage tissue engineering, Biomaterials 30 (2009) 2499-2506.

[20] S. Yodmuang, S. L. McNamara, A. B. Nover, B. B. Mandal, M. Agarwal, T. A. N. Kelly, P. H. G. Chao, C. Hung, D. L. Kaplan, G. Vunjak-Novakovic, Silk microfiber-reinforced silk hydrogel composites for functional cartilage tissue repair,

Acta Biomater. 11 (2015) 27-36.

[21] C. G. Williams, A. N. Malik, T. K. Kim, P. N. Manson, J. H. Elisseeff, Variable cytocompatibility of six cell lines with photoinitiators used for polymerizing hydrogels and cell encapsulation, Biomaterials 26 (2005) 1211-1218.

[22] B. S. Chiou, R. J. English, S. A. Khan, Rheology and photo-cross-linking of thiol-ene polymers, Macromolecules 29 (1996) 5368-5374.

[23] D. Dikovsky, H. Bianco-Peled, D. Seliktar, Defining the role of matrix compliance and proteolysis in three dimensional cell spreading and remodeling, Biophys. J. 94 (2008) 2914-2925.

[24] G. Srivastava, S. Walke, D. Dhavale, W. Gade, J. Doshi, R. Kumar, S. Ravetkar, P. Doshi, Tartrate/tripolyphosphate as co-crosslinker for water soluble chitosan used in protein antigens encapsulation, Int. J. Biol. Macromol 91 (2016) 381-393.

[25] C. K. Chen, S. C. Huang, Preparation of reductant-responsive N-maleoyl-functional chitosan/poly (vinyl alcohol) nanofibers for drug delivery, Mol. Pharmaceut. 13 (2016) 4152-4167.

[26] T. Arai, H. Ishikawa, G. Freddi, S. Winkler, M. Tsukada, Chemical modification of bombyx mori silk using isocyanates, J. Appl. Polym. Sci. 79 (2001) 1756-1763.

[27] B. N. Singh, N. N. Panda, R. Mund, K. Pramanik, Carboxymethyl cellulose enables silk fibroin nanofibrous scaffold with enhanced biomimetic potential for bone tissue engineering application, Carbohydr. Polym. 151 (2016) 335-347.

[28] J. Shao, J. Liu, J. Zheng, C. M. Carr, X-ray photoelectron spectroscopic study of silk fibroin surface, Polym. Int. 51 (2002) 1479-1483.

[29] X. Qin, J. Torgersen, R. Saf, S. Muhleder, N. Pucher, S. C. Ligon, W. Holnthoner, H. Redl, A. Ovsianikov, J. Stampfl, R. Liska, Three-dimensional microfabrication of protein hydrogels via two-photo-excited thiol-vinyl ester photopolymerization, J. Polym. Sci. Pol. Chem. 51(2013) 4799-4810.

[30] C. A. Bonino, J. E. Samorezov, O. Jeon, E. Alsberg, S. A. Khan, Real-time in situ rheology of alginate hydrogel photocrosslinking, Soft Matter 7(2011) 11510-11517.

[31] A. C. Borges, P. E. Bourban, D. P. Pioletti, J. A. E. Manson, Curing kinetics and mechanical properties of a composite hydrogel for the replacement of the nucleus pulposus, Compos. Sci. Technol. 70 (2010) 1847-1853.

[32] J. Han, Wang, K. D. Yang, J. Nie, Photopolymerization of methacrylated chitosan/PNIPAAm hybrid dual-sensitive hydrogels as carrier for drug delivery, Int. J. Biol. Macromol. 44 (2009) 229-235.

[33] Y. Shi, D. Xiong, Y. Liu, N. Wang, X. Zhao, Swelling, mechanical and friction properties of PVA/PVP hydrogels after swelling in osmotic pressure solution, Mater. Sci. Eng. C 65 (2016) 172-180.

[34] S. M. McNary, K. A. Athanasiou, A. H. Reddi, Engineering lubrication in articular cartilage, Tissue eng. Part B 18 (2012) 88-100.

[35] L. Cao, X. Fu, C. Xu, S. Yin, Y. Chen, High-performance natural rubber nanocomposites with marine biomass (tunicate cellulose), Cellulose 24 (2017) 2849-2860.

[36] F. T. Moutos, L. E. Freed, F. Guilak, A biomimetic three-dimensional woven composite scaffold for functional tissue engineering of cartilage, Nat. Mater. 6 (2007)

162-167.

[37] A. K. Gaharwar, C. P. Rivera, C. J. Wu, G. Schmidt, Transparent, elastomeric and tough hydrogels from poly (ethylene glycol) and silicate nanoparticles, Acta Biomater. 7 (2011) 4139-4148.

[38] F. Han, F. Zhou, X. Yang, J. Zhao, Y. Zhao, X. Yuan, A pilot study of conically graded chitosan-gelatin hydrogel/PLGA scaffold with dual-delivery of TGF-β1 and BMP-2 for regeneration of cartilage-bone interface, J. Biomed. Mater. Res. B 103 (2015) 1344-1353.

[39] J. Kim, B. Lin, S. Kim, B. Choi, D. Evseenko, M. Lee, TGF-β1 conjugate chitosan collagen hydrogels induce chondrogenic differentiation of human synovium-derived stem cells, J. Biol. Eng. 9 (2015) 1-11.